

Parton coalescence and the antiproton/pion anomaly at RHIC

V. Greco,¹ C. M. Ko,¹ and P. Lévai^{1,2}

¹*Cyclotron Institute and Physics Department, Texas A&M University, College Station, Texas 77843-3366, USA*

²*KFKI Research Institute for Particle and Nuclear Physics, P.O. Box 49, Budapest 1525, Hungary*

(Dated: February 8, 2008)

Coalescence of minijet partons with partons from the quark-gluon plasma formed in relativistic heavy ion collisions is suggested as the mechanism for production of hadrons with intermediate transverse momentum. The resulting enhanced antiproton and pion yields at intermediate transverse momenta gives a plausible explanation for the observed large antiproton to pion ratio. With further increasing momentum, the ratio is predicted to decrease and approach the small value given by independent fragmentations of minijet partons after their energy loss in the quark-gluon plasma.

PACS numbers: 25.75.-q, 25.75.Dw, 25.75.Nq, 12.38.Bx

Heavy ion collisions at the Relativistic Heavy Ion Collider (RHIC) provides the possibility of creating in the laboratory a plasma of deconfined quarks and gluons. One of the signatures for the quark-gluon plasma (QGP) is suppression of jet production [1]. Experimental data on high transverse momentum hadrons [2, 3], which are dominantly produced from minijet partons originated from initial hard processes between colliding nucleons, have indeed shown a large suppression compared to what is expected from the superposition of primary binary nucleon-nucleon collisions. The amount of energy loss of minijet partons, particularly gluons, is consistent with the scenario that they have traversed through a dense matter that consists of colored quarks and gluons [4, 5]. Conversions of minijet partons to high transverse momentum hadrons is usually modeled by fragmentation functions which describe how minijet partons combine with quarks and antiquarks from the vacuum to form hadrons as they separate. The parameters in the fragmentation functions can be determined by fitting the experimental data from high energy electron-positron annihilation and proton-proton collisions. Because of the presence of the quark-gluon plasma, which is lacking in proton-proton collisions, minijet partons in heavy ion collisions can also combine with quarks and antiquarks in the QGP to form hadrons. Since the momenta of quarks and antiquarks in the QGP are much smaller than those of minijet partons, these hadrons have momenta between those from the independent fragmentations of minijet partons and from the hadronization of the QGP. These intermediate momentum hadrons thus carry information about the QGP formed in relativistic heavy ion collisions.

In this letter, we shall adopt the coalescence model to study hadron production from the recombination of minijet partons with QGP partons. The coalescence model has previously been used in the ALCOR [6] and MICOR [7] models to describe hadron yields from the QGP expected to be formed in relativistic heavy ion collisions. More recently, it has been introduced in a Multiphase Transport Model (AMPT) [8] to model the hadronization of the partonic matter formed during the initial stage of

relativistic heavy ion collisions [9]. Coalescence of hard minijet partons with soft QGP partons was first introduced in Ref. [10] to predict the flavor ordering of elliptic flows of high transverse momentum hadrons. In the present study, we shall show that including hadrons from this production mechanism besides thermal hadrons from the hadronization of an expanding QGP can explain the increasing antiproton to pion ratio at low transverse momentum and comparable antiproton and pion yields at intermediate transverse momentum observed in recent experimental data from RHIC [11]. We further show that the antiproton to pion ratio decreases at large transverse momenta and approaches the small value given by the independent fragmentations of minijet partons.

We consider central Au+Au collisions (0–10%) at 200 AGeV. The transverse momentum distribution of minijet partons in midrapidity can be obtained from an improved perturbative QCD calculation [12] with a nucleon parton distribution function (PDF) that includes transverse momentum smearing. Kinematic details and a systematic analysis of pp collisions can be found in Ref. [12]. Using the GRV94 LO result for the PDF [13] and the KKP fragmentation function from Ref. [14], the measured data in the reaction $pp \rightarrow \pi^0 X$ at $\sqrt{s} = 200$ GeV can be reproduced with an average transverse momentum smearing of 1.4 GeV. To include parton energy loss in the QGP formed in the collisions, we use an effective opacity $L/\lambda = 3.5$ as extracted from fitting the spectrum of high transverse momentum pions measured at RHIC [5]. Taking the momentum cutoff $p_0 = 1.75$ GeV/c for the minijet partons, the transverse momentum spectra of minijet partons at midrapidity ($y = 0$) in central Au+Au collisions at $\sqrt{s} = 200$ AGeV are shown in Fig. 1 for the gluon (dash-dotted curve), u (solid curve) and \bar{u} (dashed curve) quarks. The d and \bar{d} quark distributions are similar to those of u and \bar{u} quarks.

The QGP partons, which dominate transverse momentum below p_0 , are taken to have a temperature $T = 180$ MeV and to occupy a volume $V = 730$ fm³. This thermal parton transverse momentum distribution is also shown in Fig. 1. Compared to the power-like minijet parton

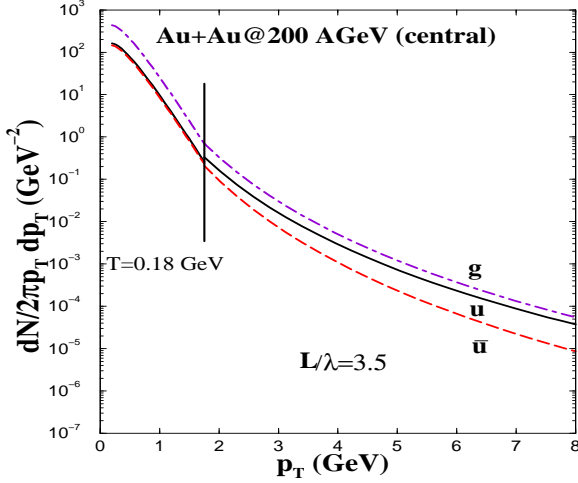


FIG. 1: Parton transverse momentum distributions at hadronization in Au+Au collisions at $\sqrt{s} = 200$ AGeV. The minijet partons with p_T greater than 1.75 GeV/c after energy loss are shown by dash-dotted curve for gluons, solid curve for u quarks, and dashed curve for \bar{u} quarks. Partons with p_T below 1.75 GeV/c are from the quark-gluon plasma at temperature $T = 180$ MeV.

spectrum, the spectrum of thermal partons is exponential. Because of scattering of minijet partons with thermal partons as they traverse the QGP, those with momenta around p_0 are expected to be thermalized with QGP partons, leading to a smooth spectrum around p_0 . In the present schematic study, we neglect this effect. The total transverse energy per unit rapidity due to both thermal and minijet partons is about 570 GeV and is consistent with that measured in experiments [15]. Most of this transverse energy comes from soft thermal partons as the contribution of minijet partons is only about 10%.

The basic equation in the coalescence model for the formation of a pion from a quark and an antiquark is similar to that for deuteron production from nucleons [16, 17, 18] and can be written as

$$\frac{dN_\pi}{d^3\mathbf{p}_\pi} = g_\pi \int d^3\mathbf{x}_1 d^3\mathbf{x}_2 d^3\mathbf{p}_1 d^3\mathbf{p}_2 f_q(\mathbf{x}_1, \mathbf{p}_1) f_{\bar{q}}(\mathbf{x}_2, \mathbf{p}_2) \times \delta^3(\mathbf{p}_\pi - \mathbf{p}_1 - \mathbf{p}_2) f_\pi(\mathbf{x}_1 - \mathbf{x}_2, \mathbf{p}_1 - \mathbf{p}_2). \quad (1)$$

In the above, $f_q(\mathbf{x}, \mathbf{p})$ and $f_{\bar{q}}(\mathbf{x}, \mathbf{p})$ are the Wigner distribution functions for quarks and antiquarks, respectively, and they are normalized to their numbers, i.e., $\int d^3\mathbf{x} d^3\mathbf{p} f_{q,\bar{q}}(\mathbf{x}, \mathbf{p}) = N_{q,\bar{q}}$. The Wigner function for the pion is denoted by $f_\pi(\mathbf{x}, \mathbf{p})$, and it is normalized as $\int d^3\mathbf{x} d^3\mathbf{p} f_\pi(\mathbf{x}, \mathbf{p}) = (2\pi)^3$. The factor g_π takes into account the probability of forming a colorless spin zero pion from spin 1/2 color quarks, e.g., $g_{\pi^+} = 1/36$ for forming a π^+ from a pair of u and \bar{d} quarks.

Assuming that quarks and antiquarks are uniformly distributed in the fireball of volume V , then the quark and antiquark Wigner functions are simply related to their momentum distributions, i.e., $f_{q,\bar{q}}(\mathbf{x}, \mathbf{p}) =$

$1/V dN_{q,\bar{q}}/d^3\mathbf{p}$. The Wigner function for a pion depends on the spatial and momentum distributions of its constituent quark and antiquark. For a schematic study, we use uniform distributions, i.e.,

$$f_\pi(\mathbf{x}, \mathbf{p}) = \frac{9\pi}{2\Delta_x^3 \Delta_p^3} \Theta(\Delta_x - |\mathbf{x}|) \Theta(\Delta_p - |\mathbf{p}|), \quad (2)$$

where Δ_x and Δ_p are, respectively, the spatial and momentum cutoffs in the phase space of quark-antiquark relative motions. The uncertainty relation then requires $\Delta_x \Delta_p \geq \hbar$.

For hadrons in midrapidity ($y = 0$), we only need to consider their transverse momentum. Since minijet partons move essentially with velocity of light, they are more likely to coalesce with comoving QGP partons, i.e., moving in the same direction, to form hadrons. This leads to the following simplified expression for coalescence of quarks and antiquarks to form pions:

$$\begin{aligned} \frac{dN_\pi}{d^2\mathbf{p}_{\pi,T}} &= g_\pi \frac{6\pi^2}{V \Delta_p^3} \int p_{q,T} dp_{q,T} p_{\bar{q},T} dp_{\bar{q},T} \\ &\times \frac{dN_q}{d^2\mathbf{p}_{q,T}} \frac{dN_{\bar{q}}}{d^2\mathbf{p}_{\bar{q},T}} \delta(p_{\pi,T} - p_{q,T} - p_{\bar{q},T}) \\ &\times \Theta(\Delta_p - |p'_{q,T} - p'_{\bar{q},T}|/2), \end{aligned} \quad (3)$$

where $p'_{q,T}$ and $p'_{\bar{q},T}$ are momenta of quark and antiquark in the center-of-mass frame of formed pion. In making the Lorentz transformation from the fireball frame to the pion frame, we use the current quark mass of 10 MeV for minijet quarks but the constituent quark mass of 300 MeV for QGP quarks due to nonperturbative effects.

The above results can be generalized to formation of protons and antiprotons from the parton distribution functions. We take the antiproton Wigner function as

$$\begin{aligned} f_{\bar{p}}(\mathbf{x}, \mathbf{y}; \mathbf{p}, \mathbf{q}) &= \frac{9\pi}{2\Delta_x^3 \Delta_p^3} \Theta(\Delta_x - |\mathbf{x}|) \Theta(\Delta_p - |\mathbf{p}|) \\ &\times \frac{9\pi}{2\Delta_y^3 \Delta_q^3} \Theta(\Delta_y - |\mathbf{y}|) \Theta(\Delta_q - |\mathbf{q}|), \end{aligned} \quad (4)$$

where $\mathbf{x} = (\mathbf{x}_1 - \mathbf{x}_2)$ and $\mathbf{y} = (\mathbf{x}_1 + \mathbf{x}_2)/2 - \mathbf{x}_3$ are the relative coordinates among three antiquarks, while $\mathbf{p} = (\mathbf{p}_1 - \mathbf{p}_2)/2$ and $\mathbf{q} = (\mathbf{p}_1 + \mathbf{p}_2 - \mathbf{p}_3)/2$ are corresponding relative momenta. As for pions, the uncertainty relation requires that $\Delta_x \Delta_p$ and $\Delta_y \Delta_q$ cannot be less than \hbar . For simplicity, we take $\Delta_x = \Delta_y$ and $\Delta_p = \Delta_q$. This leads to the following antiproton transverse momentum spectrum from coalescence of three antiquarks:

$$\begin{aligned} \frac{dN_{\bar{p}}}{d^2\mathbf{p}_{\bar{p},T}} &= g_{\bar{p}} \frac{36\pi^4}{V^2 \Delta_p^6 p_{\bar{p},T}^2} \int \prod_{i=1,3} p_{\bar{q}_i,T} dp_{\bar{q}_i,T} \frac{dN_{\bar{q}_i}}{d^2\mathbf{p}_{\bar{q}_i,T}} \\ &\times \delta(p_{\bar{p},T} - p_{\bar{q}_1,T} - p_{\bar{q}_2,T} - p_{\bar{q}_3,T}) \\ &\times \Theta(\Delta_p - |p'_{\bar{q}_1,T} - p'_{\bar{q}_2,T}|/2) \\ &\times \Theta(\Delta_p - |p'_{\bar{q}_1,T} + p'_{\bar{q}_2,T} - p'_{\bar{q}_3,T}|/2). \end{aligned} \quad (5)$$

In the above, $g_{\bar{p}}$ is the probability of forming a colorless spin 1/2 antiproton from two \bar{u} quarks and one \bar{d} quark, i.e., $g_{\bar{p}} = 1/108$. The antiquark momenta in the center-of-mass frame of formed antiproton are denoted by $p'_{\bar{q},T}$.

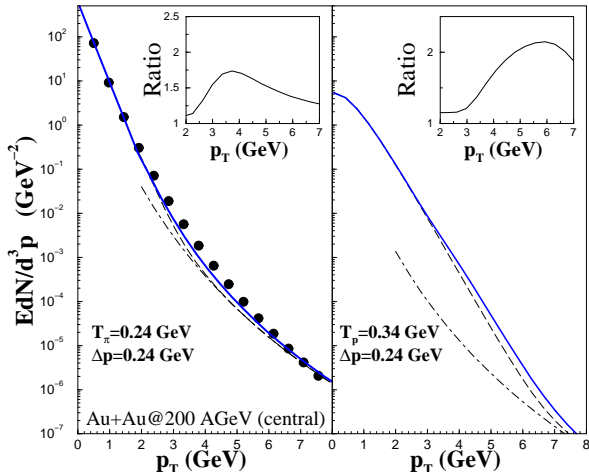


FIG. 2: Transverse momentum spectra of pions (left panel) and antiprotons (right panel) from Au+Au collisions at $\sqrt{s} = 200$ AGeV. Dashed curves are results including contributions from thermal hadrons and hadrons from independent fragmentations of minijet partons (dash-dotted curves). Adding also hadrons from coalescence of minijet partons with QGP partons gives the solid curves. Ratio of the solid to the dashed curve is given in the insets. Experimental π^0 data [19] are shown by filled circles.

We first take thermal hadrons to have exponential transverse mass ($m_T = \sqrt{m^2 + p_T^2}$) spectra with inverse slope parameter equal to 240 MeV for pions and 340 MeV for antiprotons in order to reproduce the observed low transverse momentum spectra of these particles. The larger inverse slope parameter than the QGP temperature reflects the effect due to collective transverse flow of the QGP, which increases the transverse momentum of heavier antiprotons more than that of lighter pions. The number of thermal pions is fixed by fitting the measured pion spectrum at low transverse momenta, while that of thermal antiprotons is determined by requiring that it is 0.7 of the pion number at transverse momentum of 2 GeV/c as in experimental measurements. Hard hadrons, shown in Fig. 2 by dash-dotted curves, are obtained from minijet partons using the KKP fragmentation function of Ref. [14], which has been shown to reproduce measured high transverse momentum particles at RHIC. The hadron spectra from the sum of these two contributions are shown in Fig. 2 by dashed curves. As shown in the left panel, the final pion spectrum at intermediate transverse momentum is below the experimental data from the PHENIX Collaboration [19] shown by filled circles.

To evaluate the contribution to pion and antiproton production from coalescence of minijet quarks and antiquarks with those from the QGP, the effect due to gluons is taken into account by converting them to quark-

antiquark pairs with equal probability for different flavors as assumed in the ALCOR model [6]. Using $\Delta_p = 0.24$ GeV/c corresponding to a pion size of $\Delta_x \approx 0.85$ fm, the coalescence contribution leads to a final pion spectrum, shown by the solid curve in the left panel of Fig. 2, that agrees reasonably with the experimental data. For simplicity, the same Δ_p is used to evaluate the coalescence contribution to antiproton production, and the resulting final antiproton spectrum is shown by the solid curve in the right panel of Fig. 2. From the ratio of hadron spectra with and without the coalescence contribution shown in the insets of Fig. 2, this new mechanism is seen to enhance the yields of intermediate transverse momentum pions and antiprotons by factors of about 1.7 and 2.2, respectively.

In Fig. 3, we show the ratio of antiproton to pion as a function of transverse momentum obtained with different scenarios for the antiproton spectrum but the same empirical pion spectrum shown in the left panel of Fig. 2. The dashed curve corresponds to an antiproton spectrum that includes only the thermal and perturbative ones, i.e., the dashed curve in the right panel of Fig. 2. This theoretical result is below the experimental antiproton to pion ratio given by filled squares [11] when the transverse momentum is above 2 GeV/c. Including antiproton production from coalescence of minijet partons with thermal partons enhances the ratio significantly as shown by the dashed curve with open circles, which is now above the experimental ratio.

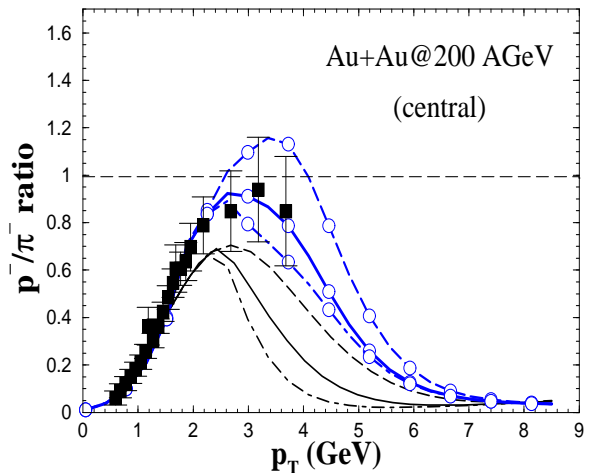


FIG. 3: Antiproton to pion ratios from Au+Au collisions at $\sqrt{s} = 200$ AGeV. Dash-dotted, solid, and dashed curves are results using, respectively, 240, 300, and 340 MeV for the inverse slope parameter of intermediate p_T antiprotons. Corresponding results including also contributions from coalescence of minijet and QGP partons are shown with open circles. Filled squares are the experimental data [11].

Since the collective flow effect is expected to diminish with increasing antiproton transverse momentum, we explore this possibility by varying the inverse slope parameter of the transverse momentum spectrum of ther-

mal antiprotons above 2.5 GeV/c. Taking the inverse slope parameter of these antiprotons to be 240 MeV, same as that for pions, the antiproton to pion ratio is shown in Fig. 3 by the dash-dotted curve and the dash-dotted curve with open circle for the cases without and with the coalescence contribution to antiproton production, respectively. In this case, coalescence of minijet and QGP partons again increases appreciably the antiproton to pion ratio at intermediate transverse momenta compared to that without this contribution, bringing the theoretical results closer to the experimental data. If the inverse slope parameter of intermediate transverse momentum thermal antiprotons is taken to have a value of 300 MeV, between those of low transverse momentum thermal pions and antiprotons, the resulting antiproton to pion ratio is shown by the solid curve and the solid curve with open circles in Fig. 3 for the cases without and with the coalescence contribution. It is seen that the experimental data can now be reproduced with the inclusion of antiproton production from coalescence of minijet partons with thermal partons.

The antiproton to pion anomaly has previously been attributed to enhanced production of antiprotons with intermediate transverse momentum from the baryon junctions in incident nucleons [20]. The possibility of enhanced baryon to pion ratio due to parton coalescence was suggested in Ref. [21]. Using a parton distribution function that is fitted to measured pion transverse momentum spectrum, a parton recombination model similar to the coalescence model indeed leads to a large antiproton to pion ratio at intermediate transverse momenta [22]. In Ref. [23], the antiproton to pion anomaly is explained by the recombination of only QGP partons with a high effective temperature. Further studies are needed to find out which of these mechanisms including ours based on the coalescence of minijet partons with partons from the quark-gluon plasma are most relevant to the observed large antiproton to pion ratio.

In summary, we have proposed a mechanism for the hadronization of minijet partons in heavy ion collisions at relativistic energies. Instead of usual independent fragmentations, in which they combine with quarks and antiquarks from the vacuum to form hadrons, these minijet partons are allowed to coalesce with thermal quarks and antiquarks from the quark-gluon plasma created in the collisions to form hadrons. Using the minijet partons predicted from the perturbative QCD, we find that this mechanism is important for production of hadrons with intermediate transverse momentum, leading to comparable antiproton and pion yields in this momentum region as observed experimentally. It further predicts that the antiproton to pion ratio would decrease as their transverse momenta become large. In this high transverse momentum region, independent fragmentations of minijet partons dominate particle production and lead to a very small antiproton to pion ratio. Confirmation of this

hadronization mechanism thus provides another evidence for the formation of the quark-gluon plasma in relativistic heavy ion collisions.

We are grateful to Su Houng Lee for useful discussions. P.L. would also like to thank discussions with G. Papp and G. Fai, and the warm hospitality of the Cyclotron Institute at Texas A&M University during his visit. This paper is based on work supported in part by the U.S. National Science Foundation under Grant No. PHY-0098805 and the Welch Foundation under Grant No. A-1358. The work of V.G. is further supported by a fellowship from the National Institute of Nuclear Physics (INFN) in Italy, while that of P.L. by Hungarian OTKA Grant Nos. T034269 and T043455.

-
- [1] X. N. Wang, Phys. Rev. C 58, 2321 (1998).
 - [2] K. Adcox *et al.* (PHENIX Collaboration), Phys. Rev. Lett. 88, 022301 (2002).
 - [3] C. Adler *et al.* (STAR Collaboration), Phys. Rev. Lett. 89, 202301 (2002).
 - [4] M. Gyulassy, P. Lévai, and I. Vitev, Phys. Rev. Lett. 85, 5535 (2000); Nucl. Phys. B 571, 197 (2000); *ibid.* B 594, 371 (2001); M. Gyulassy, I. Vitev, and X. N. Wang, Phys. Rev. Lett. 86, 2537 (2001).
 - [5] P. Lévai *et al.*, Nucl. Phys. A 698, 631 (2002); M. Gyulassy, P. Lévai, and I. Vitev, Phys. Lett. B 538, 282 (2002).
 - [6] T. S. Biró, P. Lévai, and Zimányi, Phys. Lett. B 347, 6, (1995); Phys. Rev. C 59, 1574 (1999); T. S. Biró, T. Csörgő, P. Lévai, and Zimányi, *ibid.* B 472, 273 (2000).
 - [7] P. Csizmadia and P. Lévai, Phys. Rev. C 61, 0301903 (2000); J. Phys. G 28, 1997 (2002).
 - [8] B. Zhang *et al.*, Phys. Rev. C 61, 067901 (2000); *ibid.* 62, 054905 (2000); 65, 054909 (2002); Z. Lin *et al.*, *ibid.* 64, 011902 (2001); Nucl. Phys. A 498, 375c (2002).
 - [9] Z. Lin and C. M. Ko, Phys. Rev. C 65, 034904 (2002); Phys. Rev. Lett. 89, 152301 (2002).
 - [10] Z. Lin and C. M. Ko, Phys. Rev. Lett. 89, 202302 (2002).
 - [11] K. Adcox, Phys. Rev. Lett. 88, 242301 (2002); T. Chujo, nucl-ex/209027; T. Sakaguchi, nucl-ex/0209030.
 - [12] Y. Zhang *et al.*, Phys. Rev. C 65, 034903 (2002).
 - [13] M. Glück, E. Reya, and W. Vogt, Z. Phys. C 67, 433 (1995).
 - [14] B.A. Kniehl, G. Kramer, and B. Pötter, Nucl. Phys. B 597, 337 (2001); hep-ph/0011155.
 - [15] K. Adcox *et al.* (PHENIX Collaboration), Phys. Rev. Lett. 87, 052301 (2001).
 - [16] C. Dover *et al.*, Phys. Rev. C 44, 1636 (1991).
 - [17] A. J. Baltz and C. Dover, Phys. Rev. C 53, 362 (1996).
 - [18] R. Mattiello *et al.* Phys. Rev. C 55, 1443 (1997).
 - [19] D. d'Enterria for the PHENIX Collaboration, hep-ex/0209051.
 - [20] I. Vitev and M. Gyulassy, Phys. Rev. C 65, 041902 (2002).
 - [21] S. Voloshin, nucl-ex/0210014.
 - [22] R. C. Hwa and C. B. Yang, Phys. Rev. C 67, 034902 (2003); nucl-th/0301004; nucl-th/0302006.
 - [23] R. J. Fries *et al.*, nucl-th/0301087.